

Temperature dependence of the linewidth of the first-order Raman spectrum of a MgF₂ crystal

Kazume Nishidate* and Tsutomu Sato

Department of Physics, Faculty of Science, Hirosaki University, Hirosaki, 036, Japan

(Received 6 November 1991; revised manuscript received 18 July 1992)

The first-order Raman spectrum of a MgF₂ crystal was measured at various temperatures from 300 to 903 K. In addition, the linewidth was calculated theoretically with inclusion of the cubic and quartic anharmonic terms of the repulsive part in the crystal-potential energy. These theoretical results are found to be in reasonably good agreement with experiment. The temperature dependence of the linewidth of the Raman spectrum for MgF₂ was found to arise from both the quartic and the cubic anharmonic terms; the contribution of the former was seen to become dominant at higher temperatures.

I. INTRODUCTION

Many measurements¹⁻⁹ of the temperature dependence of the linewidth and frequency of normal-mode vibrations have been carried out for various crystals. The temperature dependence of the linewidth and frequency has been studied with inclusion of the cubic or the cubic and quartic anharmonic terms in the crystal-potential energy. Skryabinskii and Ukhanov³ have shown that the linewidth of GaSb with zinc-blende structure is due only to the cubic harmonic term, while Bairamov *et al.*⁵ found the linewidth of GaP with the same structure is due to both the cubic and quartic terms. A similar behavior has been demonstrated by Jasperse *et al.*¹ for MgO and LiF crystals with the NaCl structure. However, in many of these experimental investigations¹⁻⁶ little or no physical justification were given in the choice of the frequencies used to analyze the linewidths. On the other hand, theoretical calculations have been performed by Ipatova, Maradudin, and Wallis¹⁰ and Monga, Jindal, and Pathak¹¹ on NaCl and LiF crystals, and by Elliott *et al.*¹² on some crystals with CaF₂ structure. A comparison of their theoretical results¹⁰⁻¹² with experiment shows good agreement. For the case of silicon, Balkan-

ski, Wallis, and Han⁷ have obtained a satisfactory fit to experimental data by including the cubic and quartic anharmonic terms. However, these theoretical calculations¹⁰⁻¹² have been performed mainly in the high-temperature limit and only for a few crystals. At the present time, no clear trend has been found in the relative contributions to the linewidth due to the cubic anharmonic term or the quartic term. In the hope of shedding some light on the relative contribution of these terms, we have carried out theoretical calculations and experiments at near room temperature and at higher temperatures on a MgF₂ single crystal, with rutile structure.

II. EXPERIMENT

The unit cell of the rutile structure is shown in Fig. 1, with atoms labeled according to the scheme of Porto *et al.*¹³ Cations magnesium are located at the corners and body centers of the tetrahedron, and anions (fluorine) are displaced from them by $\pm(ua, ua, 0)$ and $\pm(ua, -ua, 0)$, respectively, where a , c , and u are lattice parameters.

As has been mentioned, MgF₂ belongs to the space group D_{4h}^{14} ($P4_2/mmm$) of which the normal-mode lattice

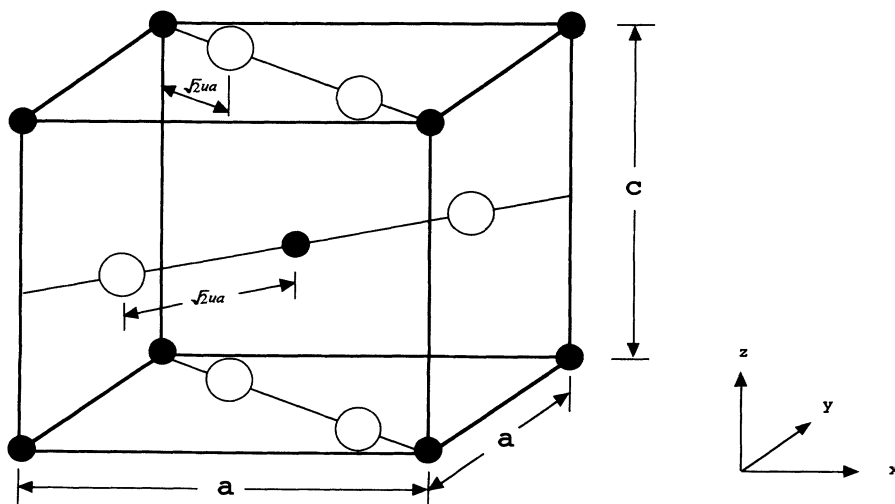


FIG. 1. Tetragonal unit cell for D_{4h}^{14} materials. Shaded and open circles represent positive and negative ions, respectively.

vibrations at the Γ point of the Brillouin zone are given by group theory (Porto *et al.*¹³) as

$$1A_{1g} + 1A_{2g} + 1A_{2u} + 1B_{1g} + 1B_{2g} + 2B_{1u} + 1E_g + 3E_u .$$

Among these, the Raman-active modes are $B_{1g}(\Gamma_3^+)$, $E_g(\Gamma_5^-)$, $A_g(\Gamma_1^+)$, and $B_{2g}(\Gamma_4^+)$. Consequently, four first-order Raman spectra are to be observed, but Raman intensities for the B_{1g} , E_g , and B_{2g} modes are weak. In the present work, the A_{1g} mode was measured.

The specimen used in the present work is a transparent crystal (prepared by Oyo Koken Co.), cut perpendicularly to the a , b , and c axes, optically polished and measured $4 \times 4 \times 5$ (c axis) mm^3 with a purity over 99.99%. The 4880-Å beam of an argon-ion laser was used as the light source for Raman excitation. The laser beam was incident on the (100) plane of the specimen in a nichrome furnace with an internal diameter of 15 mm and a length of 100 mm and the scattered light from the (010) plane was measured with a laser Raman spectrophotometer (U1-UV produced by Nippon Denshi Co.) equipped with

a photon-counting system. The observed Raman intensity is the convolution of a Lorentzian shape of the actual Raman intensity function with the response function of the spectrometer. We have done the deconvolution using the above-mentioned function. The calibration of the wavelength was carried out with a plasma line of the Argon tube. The accuracy of the wavelength was ± 0.5 Å ($\approx \pm 2 \text{ cm}^{-1}$).

III. ANHARMONIC FORCE CONSTANTS

Lattice-dynamical perturbative treatments of anharmonicity have been described in several papers;⁷⁻¹³ here we recall the expressions utilized for the calculations of the linewidths. According to Wallis, Ipatova, and Maradudin,¹⁴ the Raman linewidth 2Γ due to the cubic and quartic anharmonic terms can be expressed as follows:

$$\Gamma(\mathbf{0}, j; \Omega) = \Gamma^{(3)}(\mathbf{0}, j; \Omega) + \Gamma^{(4)}(\mathbf{0}, j; \Omega) , \quad (1)$$

where the cubic anharmonic term $\Gamma^{(3)}$ and quartic anharmonic term $\Gamma^{(4)}$ are defined by

$$\begin{aligned} \Gamma^{(3)}(\mathbf{0}, j; \Omega) = & 18 \frac{\pi}{\hbar^2} \sum_{\mathbf{q}} \sum_{j_1, j_2} |V^{(3)}(\mathbf{0}, j; \mathbf{q}, j_1; -\mathbf{q}, j_2)|^2 \{ [n(\mathbf{q}, j_1) + n(-\mathbf{q}, j_2) + 1] \\ & \times [\delta(\Omega - \omega(\mathbf{q}, j_1) - \omega(-\mathbf{q}, j_2)) - \delta(\Omega + \omega(\mathbf{q}, j_1) + \omega(-\mathbf{q}, j_2))] \\ & + 2[n(\mathbf{q}, j_1) - n(-\mathbf{q}, j_2)] \delta(\Omega - \omega(\mathbf{q}, j_1) + \omega(-\mathbf{q}, j_2)) \} , \quad (2) \end{aligned}$$

$$\begin{aligned} \Gamma^{(4)}(\mathbf{0}, j; \Omega) = & 96 \frac{\pi}{\hbar^2} \sum_{\mathbf{q}_1, \mathbf{q}_2, \mathbf{q}_3} \sum_{j_1, j_2, j_3} |V^{(4)}(\mathbf{0}, j; \mathbf{q}_1, j_1; \mathbf{q}_2, j_2; \mathbf{q}_3, j_3)|^2 \left\{ [n(\mathbf{q}_1, j_1) + 1][n(\mathbf{q}_2, j_2) + 1][n(\mathbf{q}_3, j_3) + 1] \right. \\ & - n(\mathbf{q}_1, j_1)n(\mathbf{q}_2, j_2)n(\mathbf{q}_3, j_3) \\ & \times [\delta(\Omega - \omega(\mathbf{q}_1, j_1) - \omega(\mathbf{q}_2, j_2) - \omega(\mathbf{q}_3, j_3)) \\ & \quad - \delta(\Omega + \omega(\mathbf{q}_1, j_1) + \omega(\mathbf{q}_2, j_2) + \omega(\mathbf{q}_3, j_3))] \\ & + 3\{n(\mathbf{q}_1, j_1)[n(\mathbf{q}_2, j_2) + 1][n(\mathbf{q}_3, j_3) + 1] \\ & \quad - [n(\mathbf{q}_1, j_1) + 1]n(\mathbf{q}_2, j_2)n(\mathbf{q}_3, j_3)\} \\ & \times [\delta(\Omega + \omega(\mathbf{q}_1, j_1) - \omega(\mathbf{q}_2, j_2) - \omega(\mathbf{q}_3, j_3)) \\ & \quad \left. - \delta(\Omega - \omega(\mathbf{q}_1, j_1) + \omega(\mathbf{q}_2, j_2) + \omega(\mathbf{q}_3, j_3))] \right\} , \quad (3) \end{aligned}$$

where $V^{(3)}$ and $V^{(4)}$ are the cubic and quartic anharmonic coupling coefficients, $\omega(\mathbf{q}, j)$ is the harmonic frequency at wave vector \mathbf{q} , $n(\mathbf{q}, j)$ is the thermal average of the phonon occupation number, and δ is the Dirac δ function.¹⁰

In this section we obtain an expression for the Fourier-transformed anharmonic force constants needed in the evaluation of the Raman-active phonon self-energy. Ipatova, Maradudin, and Wallis¹⁰ derived the following equation for the Fourier-transformed anharmonic force coefficients:

$$\begin{aligned} V^{(s)}(\mathbf{q}_1, j_1, \dots, \mathbf{q}_s, j_s) \\ = & \frac{1}{2} \frac{1}{S!} \left[\frac{\hbar}{2N} \right]^{s/2} N \Delta(\mathbf{q}_1 + \dots + \mathbf{q}_s) \\ & \times [\omega(\mathbf{q}_1, j_1) \cdots \omega(\mathbf{q}_s, j_s)]^{1/2} \\ & \times C_S(\mathbf{q}_1, j_1, \dots, \mathbf{q}_s, j_s) . \quad (4) \end{aligned}$$

When the potentials between magnesium and fluorine and between fluorine and fluorine are expressed as

$\phi_i(r_i)_{i=1,2}$ and $\phi_i(r_i)_{i=3,4}$, respectively, the short-range force constants are given as^{15,16}

$$A_i = \frac{2\nu}{e^2} \left[\frac{\partial^2 \phi_i(r_i)}{\partial r_i^2} \right]_0, \quad (5)$$

$$B_i = \frac{2\nu}{e^2} \left[\frac{1}{r_i} \frac{\partial \phi_i(r_i)}{\partial r_i} \right]_0,$$

where each atom's distances r_i are expressed as follows:¹⁵

$$r_1 = \sqrt{2}ua, \quad (6)$$

$$r_2 = [c^2/4 + 2(\frac{1}{2} - u)^2 a^2]^{1/2},$$

$$r_3 = [(a^2 + b^2)/4 + (2u - \frac{1}{2})^2 a^2]^{1/2},$$

$$r_4 = \sqrt{2}a(1 - u).$$

Values used for the lattice parameters are a , 4.621 Å, c = 3.052 Å, and u = 0.303. In the present calculations, only the interactions between two types of nearest-neighbor magnesium and fluorine atoms are taken into consideration, and interactions other than those between fluorine and fluorine are neglected. The cubic and quartic anharmonic potential is obtained from the third- and fourth-order derivatives of repulsive potentials, respectively.

After we performed tedious calculations according to Ipatova, Maradudin, and Wallis¹⁰ from Eq. (4) the coefficient $|C_3|^2$ due to the cubic anharmonic term was given by

$$|C_3|^2 = \frac{1}{\omega_j(0)S_3'} C_{3M} [C_{3C}^A + 2C_{3C}^B]. \quad (7)$$

Similarly $|C_4|^2$ due to the quartic anharmonic term was given by

$$|C_4|^2 = \frac{1}{\omega_j^2(0)S_4} [C_{4M}^A C_{4C}^A + C_{4M}^B \{C_{4C}^{B1} + 6C_{4C}^{B2} + 2(C_{4C}^{B3} + 6C_{4C}^{B4})\}], \quad (8)$$

where S_3' and S_4 are defined by

$$S_3' = \frac{1}{N} \sum_{\mathbf{q}} \sum_{j,j'} \omega^2(\mathbf{q},j) \omega^2(\mathbf{q},j'), \quad (9)$$

$$S_4 = \frac{1}{N^2} \sum_{\mathbf{q}_1, \mathbf{q}_2, \mathbf{q}_3} \sum_{j_1, j_2, j_3} \Delta(\mathbf{q}_1 + \mathbf{q}_2 + \mathbf{q}_3) \omega^2(\mathbf{q}_1, j_1) \times \omega^2(\mathbf{q}_2, j_2) \omega^2(\mathbf{q}_3, j_3).$$

The prime on the sum S_3' means that the terms with $j = j'$ are omitted.

Other terms are expressed as follows:

$$C_{3M} = \frac{32}{3} \frac{M_1 + M_2}{(M_1 M_2)^2},$$

$$C_{3C}^A = r_1^6 B_1'^2 + 6r_1^4 B_1' C_1' + 15r_1^2 C_1'^2,$$

$$C_{3C}^B = r_2^6 B_2'^2 + 6r_2^4 B_2' C_2' + 15r_2^2 C_2'^2,$$

$$C_{4M}^A = \frac{128}{3} \frac{M_1 + M_2}{M_1 M_2} \left[\frac{1}{M_1^3} + \frac{1}{M_2^3} \right], \quad (10)$$

$$C_{4C}^A = 2\psi_A + \psi_B + 8\psi_C + 6\psi_D + 12\psi_E + 12\psi_F,$$

$$C_{4M}^B = 32 \frac{1}{M_1 M_2} \left[\frac{1}{M_1} + \frac{1}{M_2} \right]^2,$$

$$C_{4C}^{B1} = r_1^8 A_1'^2 + 96r_1^4 B_1'^2 + 333C_1'^2,$$

$$C_{4C}^{B2} = 3r_1^6 A_1' B_1' + 4r_1^4 A_1' C_1' + 50r_1^2 B_1' C_1',$$

$$C_{4C}^{B3} = r_2^8 A_2'^2 + 48r_2^4 B_2'^2 + 45C_2'^2,$$

$$C_{4C}^{B4} = 2r_2^6 A_2' B_2' + r_2^4 A_2' C_2' + 10r_2^2 B_2' C_2'.$$

Furthermore, we set

$$\psi_A = (\psi_{A1} + 2\psi_{A2})^2, \quad \psi_B = (\psi_{B1} + 2\psi_{B2})^2,$$

$$\psi_C = (\psi_{C1} + 2\psi_{C2})^2, \quad \psi_D = (\psi_{D1} + 2\psi_{D2})^2,$$

$$\psi_E = (\psi_{E1} + 2\psi_{E2})^2, \quad \psi_F = (\psi_{F1} + 2\psi_{F2})^2,$$

$$\psi_{A1} = \frac{1}{4}(r_1^4 A_1' + 12r_1^2 B_1' + 12C_1'), \quad \psi_{B1} = 3C_1',$$

$$\psi_{A2} = t_1^4 r_2^4 A_2' + 6t_1^2 r_2^2 B_2' + 3C_2',$$

$$\psi_{B2} = t_2^4 r_2^4 A_2' + 6t_2^2 r_2^2 B_2' + 3C_2',$$

$$\psi_{C1} = \frac{1}{4}(r_1^4 A_1' + 6r_1^2 B_1'), \quad (11)$$

$$\psi_{D1} = \frac{1}{4}(r_1^4 A_1' + 12r_1^2 B_1' + 28C_1'),$$

$$\psi_{C2} = -t_1^4 r_2^4 A_2' - 3t_1^2 r_2^2 B_2',$$

$$\psi_{D2} = t_1^4 r_2^4 A_2' + 2t_1^2 r_2^2 B_2' + C_2',$$

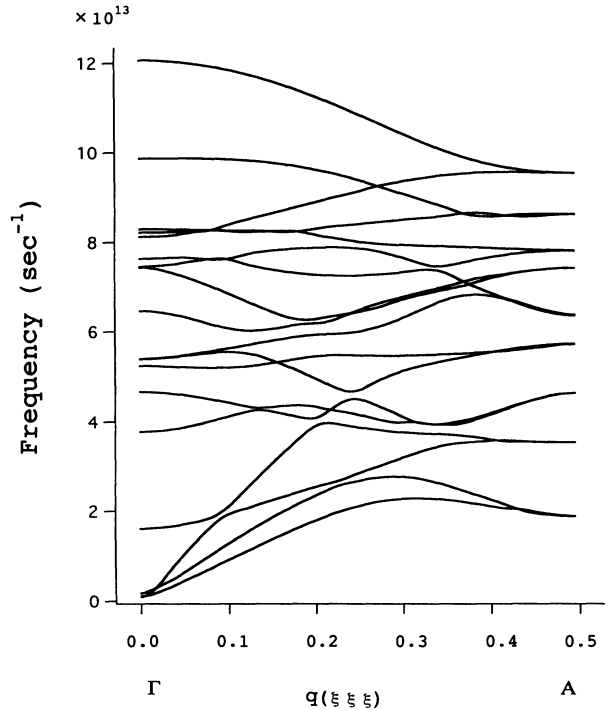


FIG. 2. Phonon dispersion curves in the direction of $q(\xi, \xi, \xi)$, calculated using the rigid-ion model according to Katiyar and Krishnan (Ref. 15) and Katiyar (Ref. 16).

TABLE I. Parameters used to calculate the phonon dispersion curves (Ref. 16).

Short-range force constants (units of $e^2/2v$)	
$A_1=71.596, A_2=72.356, A_3=4.172, A_4=16.91,$ $B_1=-9.022, B_2=-7.356, B_3=0.030, B_4=-1.54$	
Effective charge (units of e)	
$q_{Mg}/l=1.58$	$q_F/l=-0.79$

$$\psi_{E1} = \frac{1}{2}(r_1^2 B'_1 + 2C'_1), \quad \psi_{F1} = \frac{1}{2}r_1^2 B'_1,$$

$$\psi_{E2} = t_1^2 t_2^2 r_2^4 A'_2 + (t_1^2 + t_2^2)r_2^2 B'_2 + C'_2,$$

$$\psi_{F2} = -t_1^2 t_2^2 r_2^4 A'_2 - t_1^2 r_2^2 B'_2,$$

where $t_1 = (1/r_2)a(-\frac{1}{2} + u)$ and $t_2 = (a/r_2)(-c/2a)$ are dimensionless parameters that satisfy $2t_1^2 + t_2^2 = 1$. The coefficients $A'_1, A'_2, B'_1, B'_2, C'_1,$ and C'_2 involve derivatives of repulsive potentials up to second, third, and fourth order. These can be obtained in terms of our model for the anharmonic forces as

$$A'_1 = \frac{1}{r_1^4} \left[\phi^{IV}(r_1) - \frac{6}{r_1} \phi^{III}(r_1) + \frac{15}{r_1^2} \phi^{II}(r_1) - \frac{15}{r_1^3} \phi^I(r_1) \right],$$

$$A'_2 = \frac{1}{r_2^4} \left[\phi^{IV}(r_2) - \frac{6}{r_2} \phi^{III}(r_2) + \frac{15}{r_2^2} \phi^{II}(r_2) - \frac{15}{r_2^3} \phi^I(r_2) \right],$$

$$\begin{aligned} B'_1 &= \frac{1}{r_1^3} \left[\phi^{III}(r_1) - \frac{3}{r_1} \phi^{II}(r_1) + \frac{3}{r_1^2} \phi^I(r_1) \right], \\ B'_2 &= \frac{1}{r_2^3} \left[\phi^{III}(r_2) - \frac{3}{r_2} \phi^{II}(r_2) + \frac{3}{r_2^2} \phi^I(r_2) \right], \\ C'_1 &= \frac{1}{r_1^2} \left[\phi^{II}(r_1) - \frac{1}{r_1} \phi^I(r_1) \right], \\ C'_2 &= \frac{1}{r_2^2} \left[\phi^{II}(r_2) - \frac{1}{r_2} \phi^I(r_2) \right]. \end{aligned} \quad (12)$$

By using these above equations, the Raman linewidths due to the anharmonic terms were calculated.

IV. RESULTS

For the calculation of the Raman linewidth Γ of MgF_2 , the phonon dispersion curves must be calculated. Our calculations were carried out according to the method described by Katiyar and Krishnan¹⁵ and Katiyar.¹⁶ Therefore, the phonon dispersion curves were calculated with the rigid-ion model using the parameters given by Katiyar.¹⁶ The typical dispersion curves along $q(\xi, \xi, \xi)$ from these values are shown in Fig. 2. The force constants and effective charges used for the calculation of the dispersion curves are according to Table I.

The numerical values of $|C_3|^2$ and $|C_4|^2$ are $2.251 \times 10^{12} \text{ erg}^{-1}$ and $1.912 \times 10^{24} \text{ erg}^{-2}$, respectively. Both the calculated and observed values of Γ_j vs T for the A_{1g} mode are represented in Fig. 3, and the dotted curve gives the theoretical expression due to the cubic anharmonic term and slow change with temperature. Therefore, the observed curve cannot be explained using only this expression.

However, as may be evident in Fig. 3, the experimental results cannot be explained completely by the theoretical calculation described in Sec. III, but the tendency of an

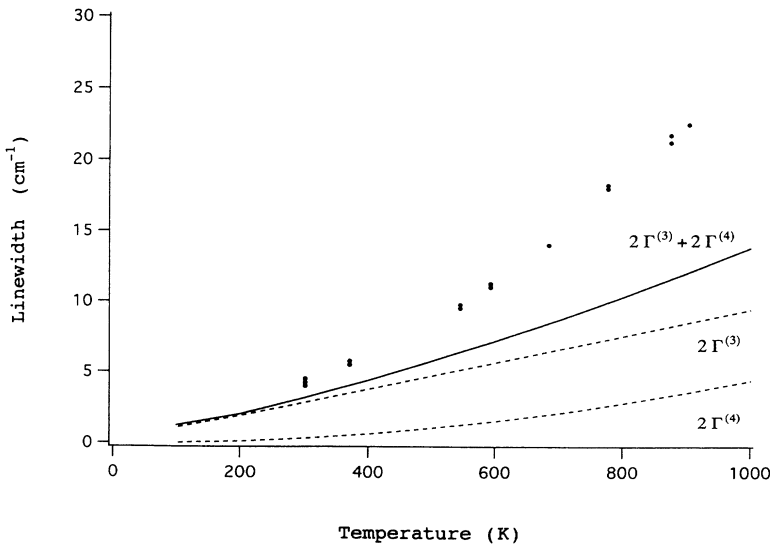


FIG. 3. Calculated curves of the cubic and quartic terms in Eqs. (2) and (3) are represented by dashed curves, and the plot of the observed values 2Γ is represented by solid circles. The dashed curve gives the calculated $2\Gamma^{(3)} + 2\Gamma^{(4)}$.

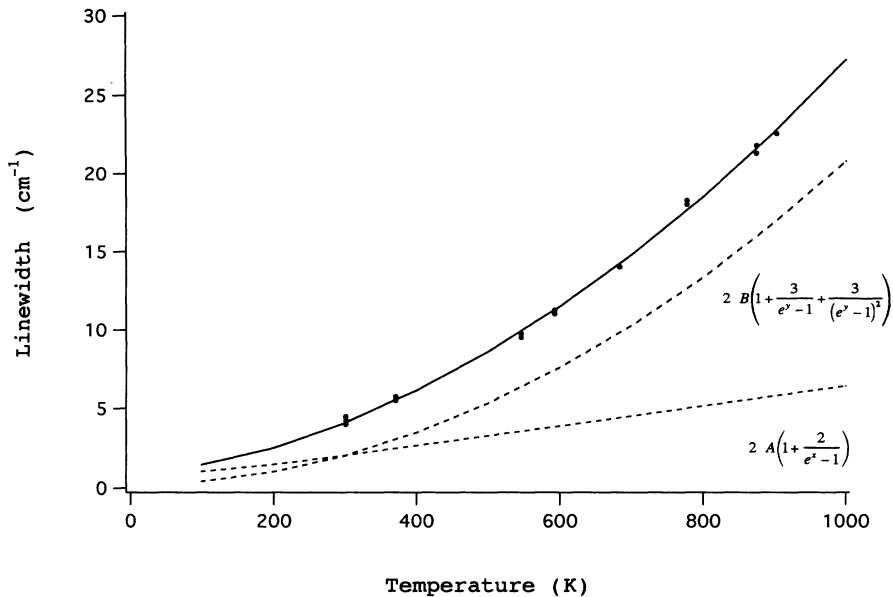


FIG. 4. The solid curve gives the theoretical fit (Ref. 7) including the cubic and quartic anharmonic terms in Eq. (13). The dashed curves represent only the cubic and quartic anharmonic contribution to the Raman linewidth. The solid circles have the same significance in Fig. 3

increased linewidth with increasing temperature and its order are reproduced very well. This demonstrates the necessity of including the quartic anharmonic term.

Now we discuss in more detail the problem of the anharmonic contribution to the linewidth as a function of temperature. With inclusion of the cubic and quartic anharmonic terms, Balkanski, Wallis, and Haro⁷ derived the following equation of the extended Klemens-Hart-Aggarwal-Lax model^{9,17} for the linewidth $2\Gamma(T)$:

$$\Gamma(T) = A \left[1 + \frac{2}{e^x - 1} \right] + B \left[1 + \frac{3}{e^y - 1} + \frac{3}{(e^y - 1)^2} \right], \quad (13)$$

where A and B are adjustable parameters, and $x = \hbar\omega_0/2k_B T$, $y = \hbar\omega_0/3k_B T$, and $\hbar\omega_0 = 410 \text{ cm}^{-1}$. We apply the above equation to the experimental result in Fig. 4 by suitably choosing constants A and B .⁷ The best values for A and B are 0.9450 and 0.2649 cm^{-1} , respectively. In Fig. 4, the solid curve gives the resulting plot of Eq. (13) and the dashed curve corresponding to only a cubic or quartic anharmonic contribution to the linewidth arising from the first or second term of Eq. (13).

It is clear from Fig. 4 that the experimental points and the solid curve agree well but the dashed curves seem to be an inadequate fit at higher temperatures. These indi-

cate the necessity of the inclusion of the cubic and quartic anharmonic terms.

V. CONCLUSION

In summary, the Raman spectrum for the A_{1g} mode of a MgF_2 single crystal has been measured at temperatures from 300 to 903 K. The values of the linewidth have been obtained at various temperatures. A theory of the Raman linewidth was derived with inclusion of the cubic and quartic anharmonic terms of the repulsive part of the crystal-potential energy. As may be seen in Fig. 3, the experimental and calculated values for the A_{1g} mode show reasonable agreement. In addition, the treatment of Balkanski, Wallis, and Haro⁷ has provided us with a very useful tool to detect the cubic or quartic anharmonic contribution to the linewidth from experiment. The application of this approach shows good agreement to experiment for the Raman linewidth in this temperature range with inclusion of the cubic and quartic anharmonic terms. The ratio B/A is found to be 0.28, and so the contribution of the quartic anharmonic term is smaller than that of the cubic one. For silicon, B/A is 0.08 (Ref. 17). In view of these results, we conclude that the temperature dependence of the linewidth of the A_{1g} mode of MgF_2 crystals can be completely explained with inclusion of the cubic and quartic anharmonic terms of the crystal-potential energy as governed by the phonon occupation number.¹⁸

*Present address: Department of Chemistry, Faculty of Science, Kanazawa University, Kanazawa, 920, Japan.

¹J. R. Jasperse, A. Kahn, J. N. Plendle, and S. S. Mitra, Phys. Rev. **146**, 526 (1966).

²T. Sakurai and T. Sato, Phys. Rev. B **4**, 583 (1971).

³I. V. Skryabinskii and Yu. I. Ukhonov, Fiz. Tverd. Tela (Len-

ingrad) **15**, 1302 (1973) [Sov. Phys. Solid State **15**, 886 (1973)].

⁴F. Gevais and B. Piriou, J. Phys. C **7**, 2374 (1974).

⁵B. Kh. Bairamov, Yu. E. Kitaev, V. K. Negoduiko, and Z. M. Khashkhozhov, Fiz. Tverd. Tela (Leningrad) **16**, 2036 (1975) [Sov. Phys. Solid State **16**, 1323 (1975)].

⁶T. Ohsaka, J. Phys. Soc. Jpn. **48**, 1661 (1980).

- ⁷M. Balkanski, R. F. Wallis, and H. Haro, *Phys. Rev. B* **28**, 1928 (1983).
- ⁸J. Menéndez and M. Cardona, *Phys. Rev. B* **29**, 2051 (1984).
- ⁹T. R. Hart, R. L. Aggarwal, and B. Lax, *Phys. Rev. B* **1**, 638 (1970).
- ¹⁰I. P. Ipatova, A. A. Maradudin, and R. F. Wallis, *Phys. Rev.* **155**, 882 (1967).
- ¹¹M. R. Monga, V. K. Jindal, and K. N. Pathak, *Phys. Rev. B* **19**, 1230 (1978).
- ¹²R. J. Elliott, W. Hayes, W. G. Kleppman, A. J. Rushworth, and J. F. Lyon, *Proc. R. Soc. London, Ser. A* **360**, 317 (1978).
- ¹³S. P. S. Porto, P. A. Fleury, and T. C. Damen, *Phys. Rev.* **154**, 522 (1967).
- ¹⁴R. F. Wallis, I. P. Ipatova, and A. A. Maradudin, *Fiz. Tverd. Tela (Leningrad)* **8**, 1064 (1966) [*Sov. Phys. Solid State* **8**, 850 (1966)].
- ¹⁵R. S. Katiyar and R. S. Krishnan, *Can. J. Phys.* **45**, 3079 (1967).
- ¹⁶R. S. Katiyar, *J. Phys. C* **3**, 1693 (1970).
- ¹⁷P. G. Klemens, *Phys. Rev.* **148**, 845 (1966).
- ¹⁸M. Born and K. Huang, *Dynamical Theory of Crystal Lattices* (Oxford University Press, New York, 1954), p. 363.